

**B.Hampel, J.Woisetschläger, N.Mayrhofer, E.Göttlich, F.Heitmeir** (2005) *Recording local density fluctuations in turbine flows using Laser Vibrometry*, Proc. 6th European Conference on Turbomachinery, Lille, pp. 950-961

# RECORDING LOCAL DENSITY FLUCTUATIONS IN TURBINE FLOWS USING LASER VIBROMETRY

*B. Hampel, J. Woisetschläger, N. Mayrhofer, E. Göttlich, F. Heitmeir*

Institute for Thermal Turbomachinery and Machine Dynamics,  
Graz University of Technology  
Graz, Austria  
ttm@ttm.tu-graz.ac.at

## ABSTRACT

**Laser vibrometers are often used for vibration diagnostics in turbomachinery research. Based on laser interferometers combined with the electronics for high-resolution signal detection they are also well suited for the recording of density fluctuations in compressible fluid flows. So, frequency spectra of turbulence can be detected close to the surface of turbine blades as well as in the main flow. While interferometric techniques usually provide integral information along the line of sight, correlation algorithms and tomographic methods give local information whenever two or more systems are combined and multi-directional observation of the flow is possible. To demonstrate the benefits, this technique is used to investigate the vortex shedding from a linear VKI-1 turbine blade cascade when Mach number (Reynolds number) is increased.**

## INTRODUCTION

Interferometric techniques are well established in vibration analysis, where interferometers enable frequency and modal analysis (so-called ‘laser vibrometers’; Lewin et al., 1990; Lewin, 1999; Tomasini, 2002). Mayrhofer and Woisetschläger (2001) presented the application of this technique to the investigation of the frequency spectra of density fluctuations in a free jet of rotational symmetry. In such a free jet a comparison of results between interferometric and probe measurements enabled a first validation of this technique for the investigation of compressible flows. Using one interferometer and one line of observation a laser-optical investigation of a turbine wake flow was performed and compared to results obtained by Particle-Image-Velocimetry (Woisetschläger et al., 2003). Recently, a free jet was studied using two laser vibrometers for a localized detection of frequency spectra of density fluctuations in compressible flows (Hampel and Woisetschläger, 2005).

The work presented herein focuses on the application of this interferometric technique for frequency analysis in a compressible flow, namely the investigation of vortex shedding in a linear turbine blade cascade in the high subsonic range. In principle the growing vortex is fed by the circulation existing in the oncoming shear layer until the vortex is strong enough to entrain fluid from the shear layer of the opposite side of the blade bearing vorticity of opposite circulation (Cicatelli and Sieverding, 1995; Cicatelli and Sieverding, 1997). When enough fluid is entrained the vortex is shed. The shedding frequency and therefore the stability of the vortex street highly depends on the boundary layer conditions. Unstable vortex shedding possibly occurs when shear layers on suction and pressure side are of different thickness, leading to a difference in formation for suction and pressure side vortices (Sieverding and Heinemann, 1990; Cicatelli and Sieverding, 1997; Sieverding et al., 2003).

Various studies have been carried out to determine different aspects of the shedding using sophisticated experimental techniques. Among them is the use of a hot-wire probe located in the wake of a blade to trigger Laser Doppler Velocimetry measurements of the periodic vortex shedding in a low speed wind tunnel (Zunino et al., 1997), as well as, the application of Particle Image Velocimetry to the investigation of wake-rotor synchronisation in a transonic compressor (Estevadoral et al., 2002)

## EXPERIMENTAL SETUP

### Turbine Blade Cascade

All tests were performed in a linear arrangement of seven VKI-1 turbine blade profiles (Kiock et al., 1986) installed into a wind tunnel with 100 x 230 mm flow cross-section. Air was continuously supplied by a centrifugal-compressor, which was part of the institutes compressor station at Graz University of Technology. Blade chord length was 58 mm, blade height 100 mm (equals channel height), spacing of blades 41.2 mm and trailing edge thickness 2.9 mm. Flow inlet and outlet conditions were continuously recorded. Exit flow Mach number  $M$  was calculated using isentropic relations, total temperature and total pressure at inlet conditions, as well as, static pressure at outlet conditions. Reynolds number  $Re$  and Strouhal number  $Str$  were based on the isentropic exit velocity and viscosity at isentropic exit conditions. Characteristic length for  $Re$  was the chord length and for  $Str$  the trailing edge thickness. During data recording Mach and Reynolds numbers were continuously displayed to control the compressor station. Reference measurements done at this profile by Laser Doppler Velocimetry indicated a turbulence level in velocity of 2% at flow inlet.

### Laser Vibrometer

The laser vibrometers used (Polytec OVD 353 mid-range Laser Vibrometers with OFV-3001 controllers and OVD-02 velocity decoders) were arranged in different ways around the test section. The setups used are explained in Fig. 1.

In Fig. 1a only one vibrometer was recording integral values of density fluctuations. Here, the laser beam was parallel to the trailing edge of the blade and was traversed into different positions along the blade surface, through the main flow and downstream the trailing edge (see also Woisetschläger et al., 2003). A surface mirror was used to reflect the beam back into the vibrometer. Beside the mid-range objective of the vibrometer a lens of – 40 mm focal length collimated the beam down to a diameter of approximately 1.5 mm (Gaussian beam diameter). For frequency analysis the vibrometer signal was fed into a NI4551 dynamic signal analyser board, allowing two channels of online Fast-Fourier-Transform (FFT) up to a bandwidth of 95 kHz at 950 lines or a continuous recording of two time signals. For each frequency spectrum a linear rms average of 2000 FFTs was performed, with a sampling rate of 204.8 kHz and 2048 values for each FFT. Additionally, frequency spectra of the mirror itself were recorded, resulting in the observation that frequencies lower than 4 kHz were also caused by vibrations (geometrical change of path length) and are not necessarily related to flow phenomena. For all other frequencies the geometrical path of the laser beam was kept constant, then only changes in density altered the optical path.

Since changes in the optical path due to changes in density delay or advance the phase front of light, these changes in phase  $\Phi'(t)$  can be related to fluctuations in density  $\rho'(z, t)$  along the optical path  $z$  and during time  $t$  by

$$\Phi'(t) = \frac{4\pi}{\lambda} G \int \rho'(z, t) dz \quad , \quad (1)$$

with  $\lambda$  the wavelength of laser light (He-Ne laser) and  $G$  the Gladstone-Dale constant ( $2.2563 \times 10^{-4} \text{ m}^3/\text{kg}$ ). For a laser vibrometer the signal voltage  $U(t)$  recorded is now linked to the phase fluctuations by

$$\mathbf{FT}\left\{\Phi'(t)\right\} = \frac{1}{j 2\pi f} \frac{4\pi}{\lambda} k_{\text{vib}} \mathbf{FT}\left\{U(t)\right\} \quad (2)$$

with  $f$  the frequency,  $k_{\text{vib}}$  the calibration factor of the vibrometer,  $j$  the imaginary unit and  $\mathbf{FT}$  denoting the Fourier transform. By applying eq. 1 the frequency spectrum of the density fluctuations are derived

$$\mathbf{FT}\left\{\rho'(t)\right\} = \frac{1}{j 2\pi f} k_{\text{vib}} \frac{1}{G \Delta z} \mathbf{FT}\left\{U(t)\right\} \quad , \quad (3)$$

with the hypothesis of a uniform density distribution over the blade height  $\Delta z$  (relevant optical path in the flow field between the two windows on both sides of the flow). This hypothesis requires a planar type of flow. Additionally, a slightly smaller signal amplitude of density fluctuations in the frequency range above 40kHz was observed compared to measurements done with fast pressure probes, which is due to the averaging effect of eq. 1 on small turbulent structures (Mayrhofer and Woisetschlager, 2001). This averaging effect is identical to the one observed with Schlieren technique and holographic interferometry.

In Fig. 1b an arrangement with two laser vibrometers is shown. For this arrangement the correlation between both signals  $U_1(t)$  (first vibrometer) and  $U_2(t)$  (second vibrometer) gives a more localized value of the frequency spectra of density fluctuations

$$\left(\mathbf{FT}\left\{\rho'(t, x, y, z)\right\}\right)^2 = \left(\frac{1}{j 2\pi f} k_{\text{vib}} \frac{1}{G \Delta z}\right)^2 \mathbf{FT}\left\{U_1(t)\right\} \mathbf{FT}^*\left\{U_2(t)\right\} \quad , \quad (4)$$

with  $x$ ,  $y$  and  $z$  the coordinates in space representing the crossing point of both laser beams.  $\Delta z$  is now a spatial correlation parameter derived from comparison of integral data for each of the vibrometers (see eq. 3) and local data from eq. 4. The asterisk (\*) denotes the complex conjugate. It has to be mentioned that eq. 4 used for the cross-correlation of two signal spectra is only valid if a linear rms average of a high number of FFTs is used (in our case 2000 FFTs).

The flow field is scanned by the crossed laser beams of the two vibrometers. Under certain circumstances artifacts might occur in the scanned fields especially when standing waves are present. In these cases the density fluctuations might correlate not only in the crossing point of the two laser beams. For these positions and frequencies the phase of the cross-correlation spectra is different to zero indicating a spatial distance of correlated structures from the crossing point and filter functions can be applied.

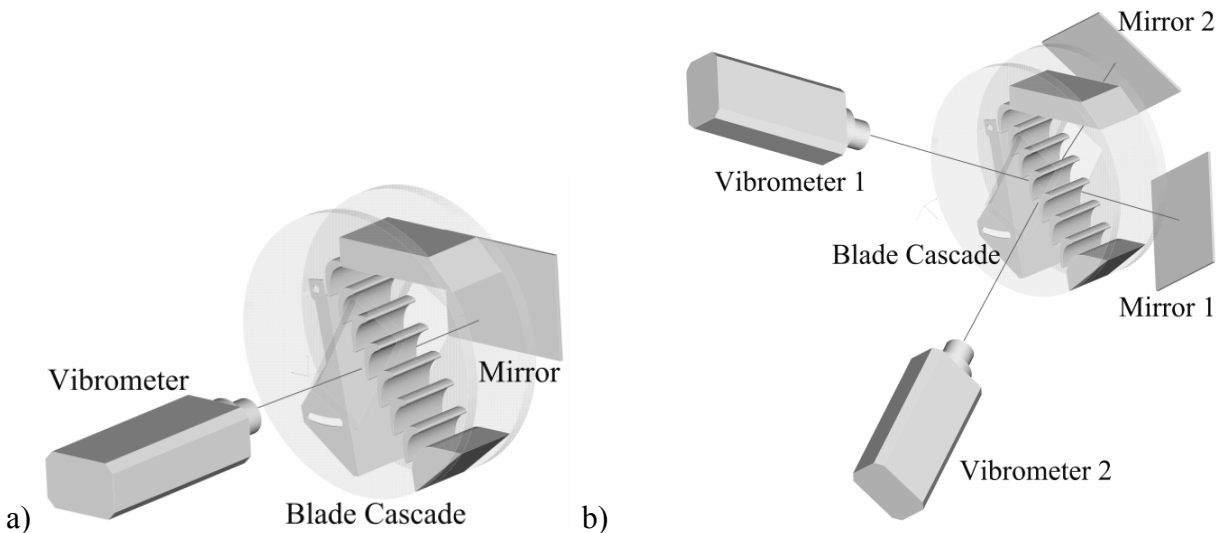


**Fig. 1** Experimental setup. **a)** shows the configuration using one laser vibrometer (integral data) and **b)** the configuration with two laser vibrometers for a better localization of the recorded density fluctuations.

Due to the discrete FFT performed by the analyser board the voltage signal in principle is ‘voltage per frequency interval’ (here, in all measurements 100Hz), so that the density fluctuation presented in the results is ‘density fluctuation per frequency interval’. In all results the *magnitude* of eqs. 3 and 4 is displayed.

### Holographic interferometry

Holographic interferometry was applied to perform a ‘modal analysis’ at the frequencies of interest. The setup is shown in Fig.2 and used a ruby laser (Lumonics HLS2) as light source. The laser was pulsed twice during one period of density change to select the frequency of interest. The interference pattern visible in the holographic interferogram of the flow then represents isolines of density change at a given frequency (e.g. Merzkirch, 1987).

A acousto-optical modulator (Steinbichler) controlled the two reference beams. This setup enabled so-called ‘phase-stepped’ holographic interferometry to obtain sub-fringe resolution. The final result can then be plotted as phase map  $\Phi'(\Delta t, x, y)$  with  $x$  and  $y$  the coordinates perpendicular to the laser beam and  $\Delta t$  the time delay between the two laser pulses (here  $2 \cdot \Delta t$  equals  $1/f$  for the frequency of interest). Finally, eq. 1 was applied to obtain the amplitude of density change between the two pulses (see e.g. Hipp et al., 2004).

This technique needed a much higher effort to scan through all frequencies compared to the laser vibrometer. In this work, holographic interferometry was used only for the visualization of a few frequencies of special interest.

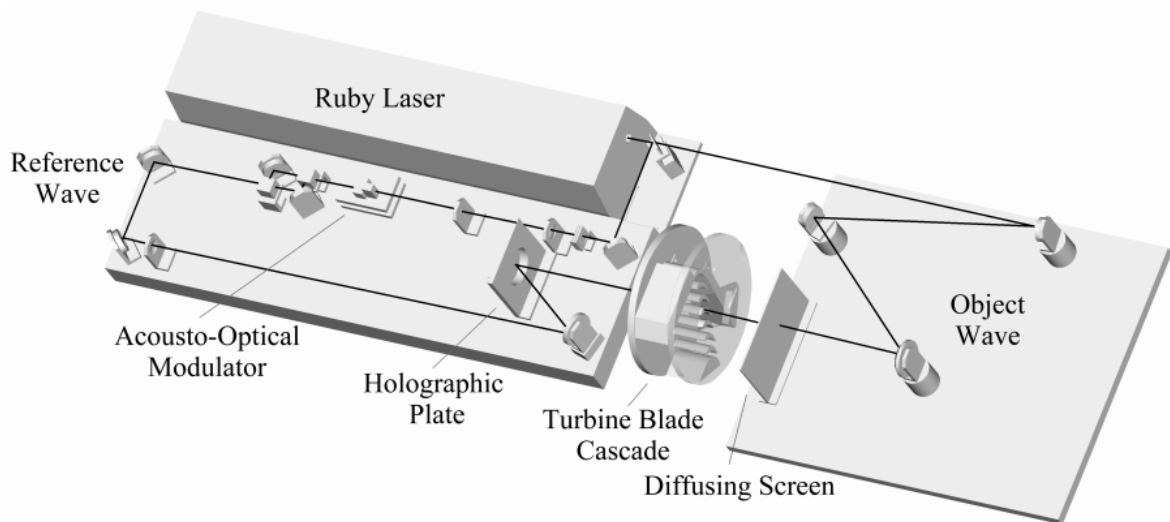


**Fig. 2** Setup for holographic interferometry. In this work, holographic interferometry was used only for the visualization of a few frequencies of special interest.

## RESULTS

### Vortex Shedding Frequency Spectra

In a first step one laser vibrometer was used to record (integral) frequency spectra of density fluctuations in the wake of the turbine blade while the Reynolds number was varied between  $2.9 \times 10^5$  and  $11 \times 10^5$  corresponding to a change in exit Mach number  $M$  from 0.24 to 0.78. These density fluctuations were caused by the vortex shedding process. For this investigation the laser beam was in a position close behind the trailing edge. The result is given in Fig. 3 and is also discussed in Woisetschläger et al., 2003. For 37 different Reynolds numbers frequency spectra were recorded and these spectra are presented along the ordinate in terms of Strouhal number.

At Reynolds numbers up to  $7 \times 10^5$  (range A in Fig. 3b) shedding frequency was above 0.3 indicating a fully laminar boundary layer shedding at the trailing edge. At  $Re = 7 \times 10^5$  the overall

magnitude of density fluctuations suddenly increased, indicating the start of boundary layer transition.

In range B (up to approximately  $Re = 9.5 \times 10^5$ ; see Fig. 3) vortex shedding took place mainly at two frequencies. (positions 1 and 2 in Fig. 3). Also higher harmonics (hh) were observed. From additional recordings by Particle Image Velocimetry it is known that in range B the frequency of vortex shedding changes between these two frequencies in the course of time (see Woisetschläger et al., 2003). Early work by Sieverding and Heinemann, 1990, found the lower frequency plateau (position 1 in Fig. 3) when a squared trailing edge was used, which caused immediate transition of the separating transitional boundary layer, while a rounded trailing edge caused shedding only at the higher frequency (position 2 in Fig. 3). In the work presented here, both frequencies were present, indicating abrupt changes in the state of the boundary layer, randomly switching between more laminar and fully turbulent state. A possible reason for this difference might be the slightly higher level of inlet turbulence used in this work (2% turbulence level in velocity). Another reason might be the higher Reynolds number at a given Mach number used in the tests presented here compared to the experiments done by Sieverding and Heinemann, 1990.

Finally, in range C (above  $Re = 9.5 \times 10^5$ ; see Fig. 3) only one shedding frequency was present ( $Str = 0.25$ ) indicating fully turbulent boundary layer conditions. Again, higher harmonics are present.

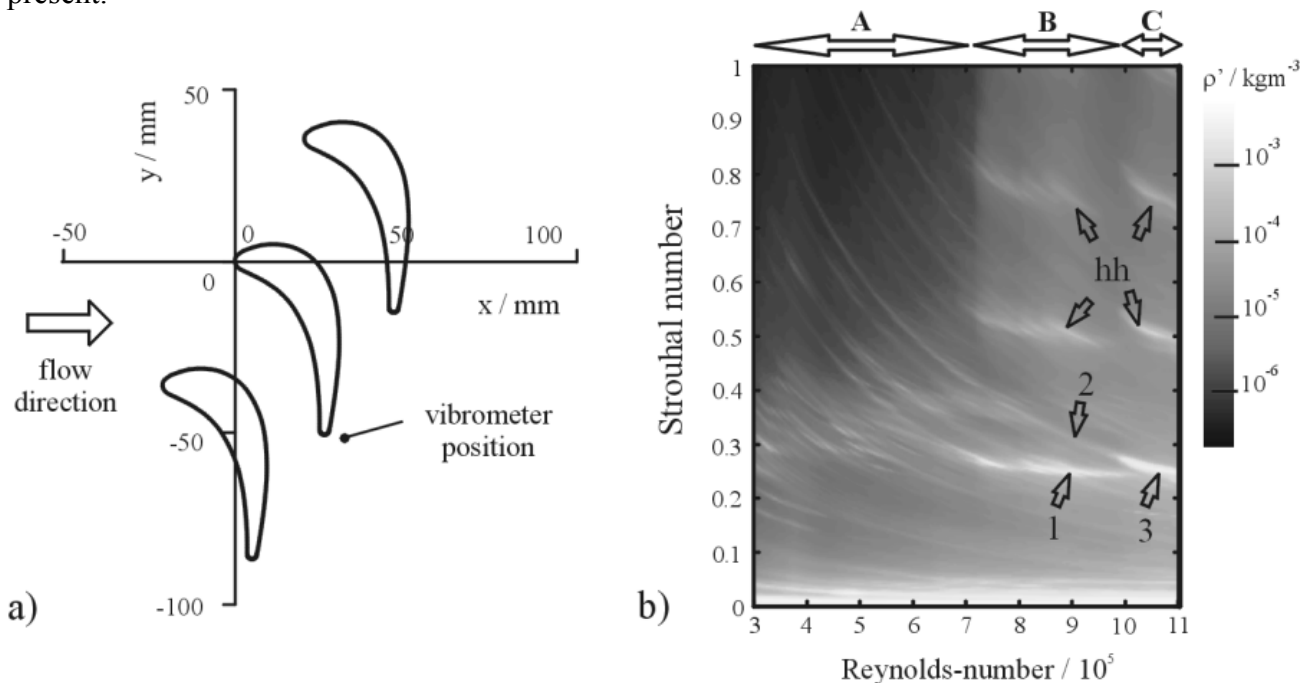


**Fig. 3** Frequency spectra of density fluctuations in the vicinity of the trailing edge of the turbine blade profile. **a)** gives the position of the laser beam and **b)** the frequency spectra of density fluctuations as function of Reynolds number (the spectra are plotted along the ordinate in terms of Strouhal number). Pronounced frequencies caused by vortex shedding are marked by numbers, hh indicate higher harmonics to these frequencies.

### Boundary Layer Condition

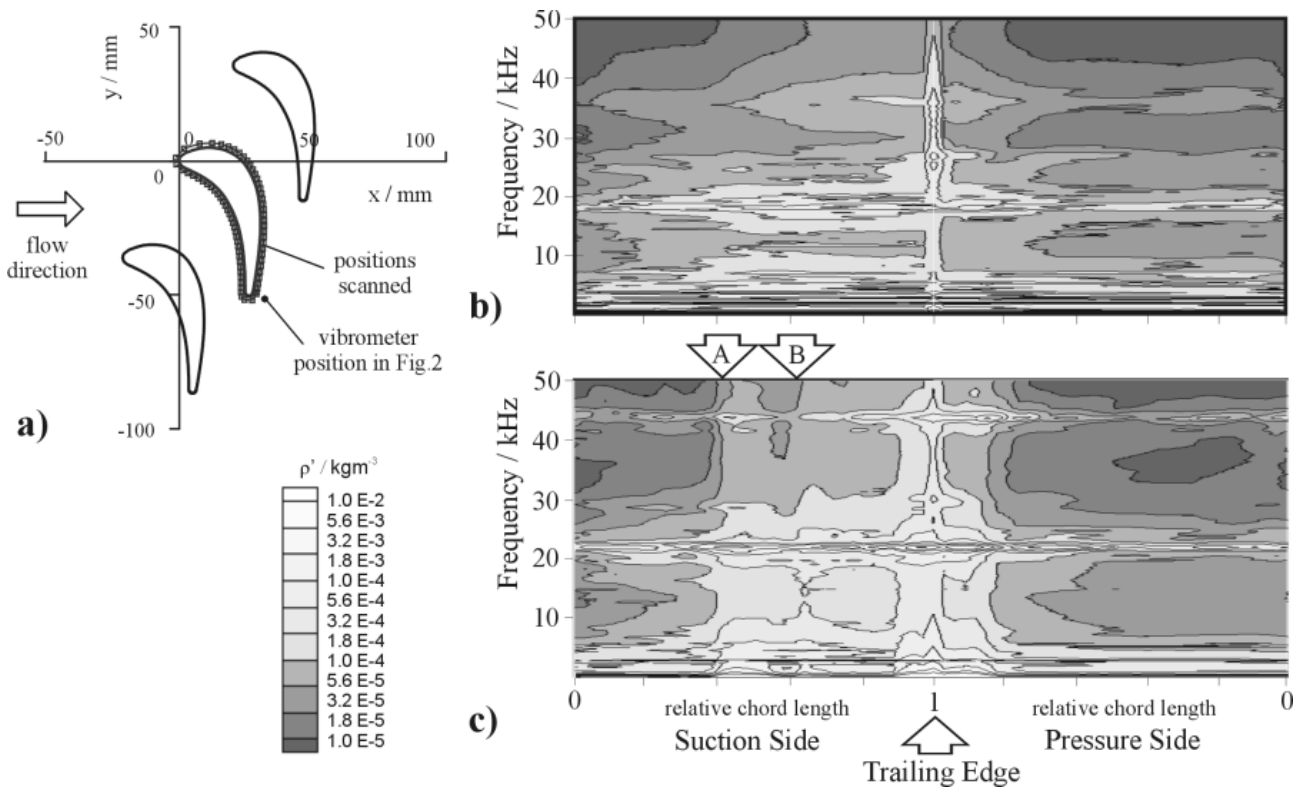
In a second step one laser vibrometer was used to record frequency spectra of density fluctuations along the surface of the turbine blade (integral data; the center of the laser beam was scanning 1.5 mm above the steel surface, which was polished).

Fig. 4b gives the frequency spectrum for different positions along the suction and the pressure side of the turbine blade at a  $M = 0.6$  and  $Re = 8.1 \cdot 10^5$ . The vortex shedding frequency was approximately 18 kHz ( $Str = 0.27$ ). Density fluctuations at this frequency were observed nearly all over the surface of the blade. A higher harmonic became visible at the trailing edge as well as some

frequencies below 6 kHz. The higher harmonic as well as the lower frequencies were more confined to the rear part of the suction side. Vertical lines at frequencies below 4 kHz stretching over all positions with nearly the same magnitude were caused by rigid body vibrations.

Fig. 4c presents the frequency spectrum for different positions along the suction and the pressure side of the turbine blade at a  $M = 0.77$  and  $Re = 10.9 \cdot 10^5$ . The dominant vortex shedding frequency was at about 22 kHz ( $Str = 0.25$ ). An higher harmonic was visible as well as some frequencies below 6 kHz. Pos. A in Fig. 4c indicates an increase of the magnitude of density fluctuations over all frequencies starting at about 50% chord length on the suction side. These complex structures point towards transitional structures randomly changing between laminar and fully turbulent conditions with some sort of relaminarisation between positions A and B. The transition on the pressure side was more confined to the vicinity of the trailing edge.

Current unsteady numerical simulations have given a first indication that pressure waves originate from shedding vortices at the blades in the cascade. These pressure waves (acoustic waves) mainly influence the suction side of the neighboring turbine blades, causing boundary layer transition in the rear part of the suction side. These wave were detected throughout the flow field and were therefore visible all over the surface of the blade with decreasing magnitude towards the leading edge.



**Fig. 4** Frequency spectra of density fluctuations recorded 1.5 mm above the surface of the turbine blade profile. **a)** gives the positions scanned, **b)** is the frequency spectrum recorded at  $Re = 8.1 \cdot 10^5$  ( $M = 0.6$ ), **c)** was recorded at  $Re = 10.9 \cdot 10^5$  ( $M = 0.77$ ). Positions A and B indicate a sudden increase of the magnitude of density fluctuations over all frequencies.

### Local Density Fluctuations

Finally, the flow field was scanned with one (integral data) and with both vibrometers (local data) to perceive information on the unsteady interactions taking place during the shedding process.

Fig. 4b presents the magnitude of the local density fluctuations as recorded with both vibrometers (Fig. 1b) at three different frequencies (2 kHz, 22 kHz, 44 kHz). Fig. 5c gives the magnitude of the density fluctuations in the flow channel at four different frequencies (2 kHz, 20.5

kHz, 22 kHz and 44 kHz; integral data using one vibrometer, see Fig. 1a). All data were recorded at  $Re = 10.9 \times 10^5$  ( $M = 0.77$ ). At this Mach number vortex shedding took place at a frequency of 22 kHz ( $Str = 0.25$ ). The pressure changes linked to the shedding process caused pressure waves propagating throughout the flow field. In Fig. 5b as well as in Fig. 5c density fluctuations with high amplitude were present at this frequency of 22 kHz throughout the flow field. These fluctuations were most pronounced in the vicinity of the trailing edges and have a slightly lower value in the middle of the flow channel (position B in Figs. 5b and 5c).

Using interferometric techniques density and density changes were detected. While the shedding process produced one clockwise and one counter-clockwise rotating vortex during one period of vortex shedding, the laser interferometer detected a twice as high frequency due to the decrease of density in the center of both vortices. While the pressure waves caused by the shedding process were observed at 22 kHz, the vortex street was therefore visible at 44 kHz (position A in Figs. 5b and 5c). The pressure waves caused by the shedding vortices propagated throughout the

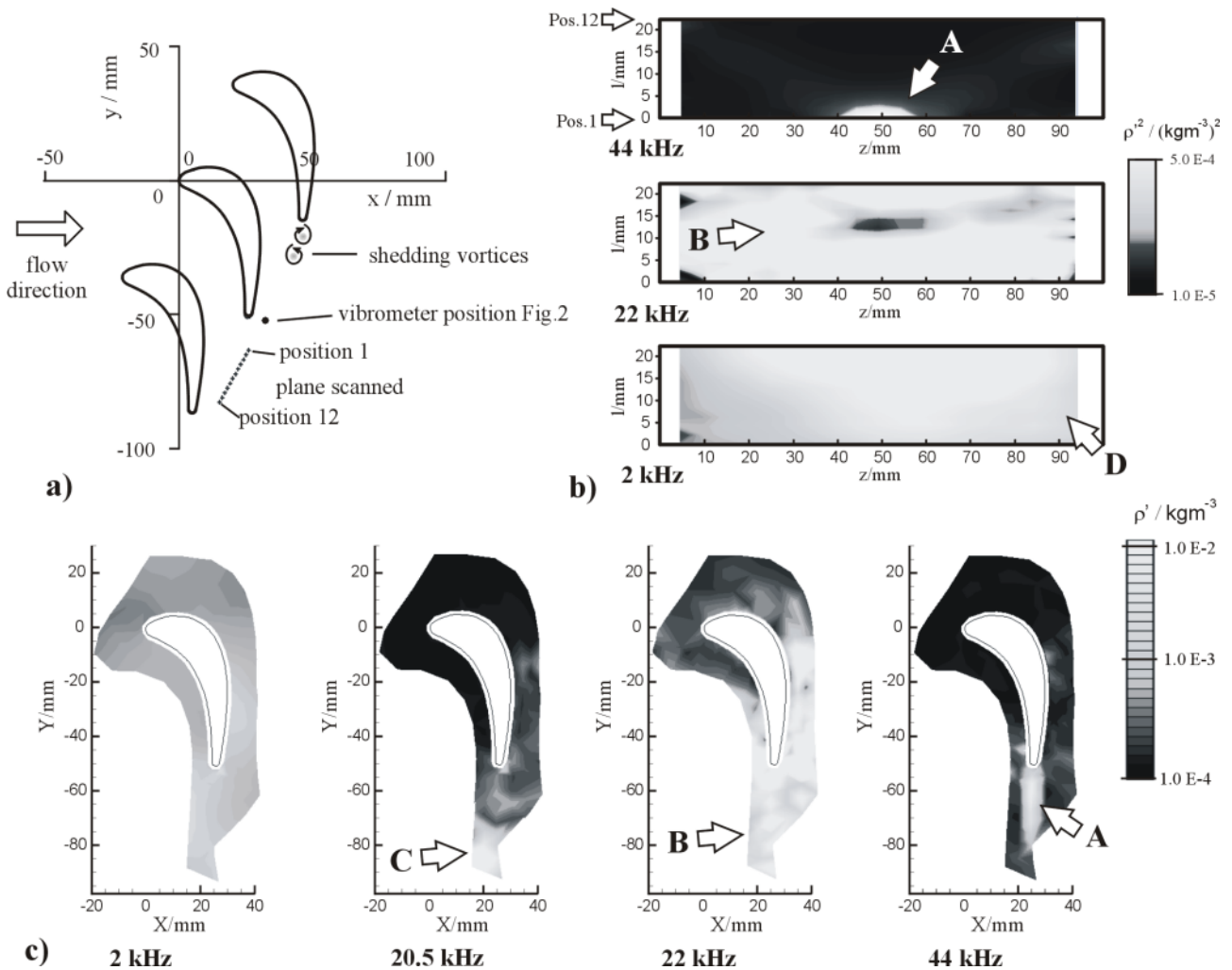


**Fig. 5** Density fluctuations recorded at given frequencies throughout the flow field. **a)** gives the positions scanned, **b)** presents the magnitude of the local density fluctuations as recorded with both vibrometers (Fig. 1b) at three different frequencies. z direction is in the direction of the blade height (100 mm). **c)** gives the magnitude of the density fluctuations in the flow channel at four different frequencies (integral data using one vibrometer, see Fig. 1a). All data were recorded at  $Re = 10.9 \times 10^5$  ( $M = 0.77$ ). Positions A mark the vortex street, B structures in the pressure-wave field, C pressure waves emitted from the neighboring blade and D higher level of turbulence probably caused by pressure probes upstream the cascade



flow field, however, the shedding vortices had the highest amplitude in the center of the blade cascade (at midspan of the turbine blades, Figs. 5b and 5c, position A). This is due to the influence of the two glass windows on both sides of the channel onto the flow.

At the lower neighboring blade a slightly different shedding frequency was observed (20.5 kHz, position C in Fig. 5c). One possible reason is that periodic conditions in the blade cascade were obtained by adjusting a tailboard visible in Figs 1a and 1b. This procedure is always error-prone and might explain the small difference in shedding frequency.

The beating frequency between the two shedding frequencies was between 1.5 and 2 kHz. This frequency was detected in the flow field and is presented in Fig. 5b and 5c (2 kHz). It was observed having its highest amplitude between the trailing edges of neighboring blades (Fig. 5c, 2 kHz).

When looking at the spatially resolved density fluctuations at 2 kHz in Fig. 5a a slight increase in magnitude can be observed towards the rear part of the cascade (position D at 70 to 90 mm in z direction). This higher level of density fluctuations can also be observed in the local recordings at 22 kHz, although it is not as pronounced. There is strong evidence that the pressure and temperature probe upstream the turbine blade cascade caused a slight increase in turbulence visible in these recordings in Fig.5b.

### **Visualization by Holographic Interferometry**

As with one vibrometer, holographic interferometry provided integral data along the path of the laser light beam. While the laser vibrometer recorded the full spectrum of density fluctuations in a single point in space, the holographic interferometry provided the density distribution over the whole flow field but for one frequency only.

Since the frequency analysis of the *vibrometer signals* included an averaging process, the *magnitude* of the density fluctuations at given frequencies were presented in Figs. 3 to 5. Therefore, bright areas indicate intense density fluctuations in these results, in dark areas there are little or no fluctuations present at this frequency.

*Holographic interferometry* now compared the phase shift of the light wave in two sequenced instants of time and displayed the *positive and negative amplitude* of the oscillation. Fig. 6 shows the recording for the two frequencies at 22 kHz (Fig 6a) and 44 kHz (Fig 6b). In Fig. 6 one light pulse recorded the flow field at the maximum, the second at the minimum amplitude of density change (with a proper chosen time delay between the two pulses the frequency was selected). The result is zero if nothing changed (mid-grey levels in Fig.6). A density increase will show up as positive amplitude (bright areas in Fig. 6), a density decrease as negative amplitude (dark areas in Fig. 6). At 44 kHz (Fig. 6b) the shedding vortices were clearly identified.

At 22 kHz (Fig. 6a) the pressure waves emitted by the vortex shedding process were observed during interaction with the boundary layer on the suction side of the neighboring blade (wave reflection by the surface). This position was clearly identified when the laser vibrometer scanned around the surface of the turbine blade (position marked by A in Fig. 4).

When this pressure wave propagates towards the trailing edge of the next blade it starts to interfere with the one emitted by the trailing edge of the neighboring blade. Due to this interference, there are areas with stronger or weaker magnitude of density fluctuations at this frequency throughout the flow field as it was observed in the field scan of the vibrometers (e.g. position B in Figs. 4b and 4c).

As seen in the recordings at lower Mach and Reynolds number in Fig. 4a, this influence of the suction-side boundary layer by the vortex shedding of neighboring blades starts when the density fluctuations become dominant in the compressible flow.

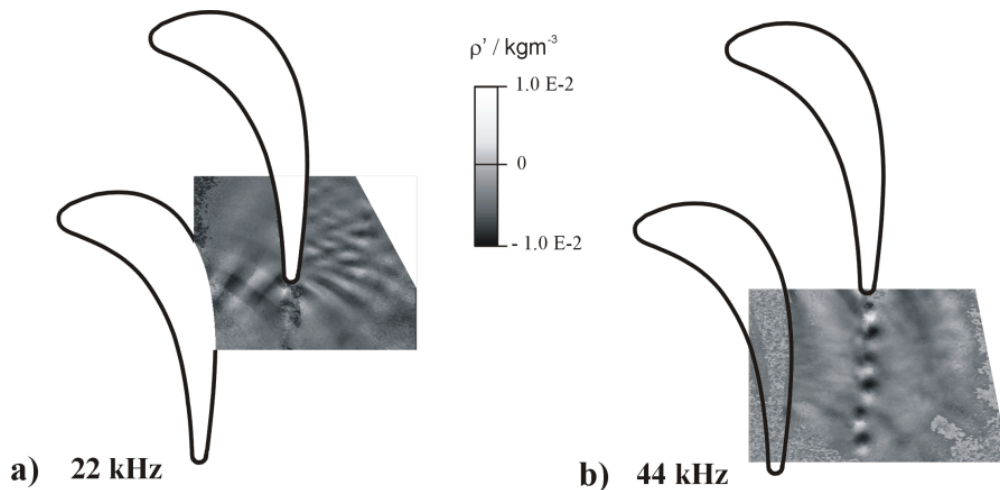


**Fig. 6** Density fluctuations recorded using holographic interferometry at a) 22 kHz and b) 44 kHz. In this instantaneous recording bright areas indicate positive amplitude and dark areas negative amplitude in density change at this frequency.

## CONCLUSIONS

Laser vibrometers (laser interferometers) allow direct observation of density fluctuations up to high frequencies, do not depend on tracer particle movement and do not interact with the flow field. Therefore, commercially available laser vibrometers enable the investigation of the frequency spectrum of unsteady flow processes. Additionally, the combination of single vibrometers allow the local observation of density fluctuations to identify the related structures in the flow field. In this work this powerful tool was applied to observe and discuss the vortex shedding and the related processes taking place in the vicinity of a VKI-1 turbine blade profile. This turbine blade is well covered in literature, so the strength of this measurement technique can be demonstrated more easily.

## ACKNOWLEDGEMENTS

This work was made possible by the Austrian Science Fund (FWF) within grant Y57-TEC (Non-intrusive Measurement of Turbulence in Turbomachinery). We also acknowledge the support of Dr. Pirker in the operation of the compressor station and Mr. Pieringer (TU-Graz) for the personal communications regarding the unsteady three-dimensional numerical simulation of the VKI-1 flow field.

## REFERENCES

- Cicatelli G, Sieverding CH (1995)** A Review of the Research on Unsteady Turbine Blade Wake Characteristics, AGARD PEP 85th Symposium on Loss Mechanisms and Unsteady Flows in Turbomachines, Derby
- Cicatelli G, Sieverding CH (1997)** The Effect of Vortex Shedding on the Unsteady Pressure Distribution Around the Trailing Edge of a Turbine Blade, ASME Journal of Turbomachinery, 119:810-819
- Estevadoral J, Gogineni S, Goss L, Copenhaver W, Gorrell S (2002)** Study of Wake-Blade Interactions in a Transonic Compressor using Visualisation and DPIV, ASME Journal of Fluids Engineering, 124:166-175
- Hampel B, Woisetschlager J (2005)** Spatially Resolved Frequency Analysis of Turbulent Compressible Flows by Laser Vibrometry, in preparation for Exp. Fluids

- Hipp M, Woisetschläger J, Reiterer P, Neger T** (2004) Digital Evaluation of Interferograms, *Measurement*, 36:53-66
- Kiock R, Lehthaus F, Baines NC, Sieverding CH** (1986) The Transonic Flow Through a Plane Turbine Cascade as Measured in Four European Wind Tunnels, *ASME Journal of Engineering for Gas Turbines and Power*, 108:277-284
- Lewin AC, Mohr F, Selbach H** (1990) Heterodyn-Interferometer zur Vibrationsanalyse. *Technisches Messen* 57(9):335-345
- Lewin A** (1999) New compact laser vibrometer for industrial and medical applications. In: Tomasini EP (ed) *Third International Conference on Vibration measurements by laser techniques*, SPIE Proc Series 3411: 61—67
- Mayrhofer N, Woisetschläger J** (2001) Frequency Analysis of Turbulent Compressible Flows by Laser Vibrometry, *Experiments in Fluids*, 31: 153-161
- Merzkirch W** (1987) *Flow Visualization*, Academic Press, Orlando
- Woisetschläger J, Mayrhofer N, Hampel B, Lang H, Sanz W** (2003) Laser-optical Investigation of turbine wake flow, *Exp.Fluids*, 34: 371-378
- Sieverding CH, Heinemann H** (1990) The Influence of Boundary Layer State on Vortex Shedding From Flat Plates and Turbine Cascades, *ASME Journal of Turbomachinery*, 112:181-187
- Sieverding CH, Hugues R, Dese Jean-Michel** (2003) **Turbine Blade Trailing Edge Flow Characteristics at High Subsonic Outlet Mach Number**, *ASME Journal of Turbomachinery*, 125:298-309
- Tomasini EP** Ed. (2002) *Fifth International Conference on Vibration Measurements by Laser Techniques: Advances and Applications*, 18-21 Juni 2002, Ancona, Italy, *Proceedings SPIE*, Vol 4827, Bellingham, Washington
- Zunino P, Ubaldi M, Campora U, Ghiglione A.** (1997) An Experimental Investigation of the Flow in the Trailing Edge Region of a Turbine Cascade, *Proceedings of 2 nd European Conference on Turbomachinery - Fluid dynamics and Thermodynamics*, Antwerpen, 247-254